# Numerical coalescence of chaotic trajectories

**Bruce N Roth**[1] and **Michael Wilkinson**[2,3]

[1] Private address
[2] School of Mathematics and Statistics, The Open University, Walton Hall, Milton Keynes, MK7 6AA, United Kingdom

E-mail: m.wilkinson@open.ac.uk

## Abstract

Pairs of numerically computed trajectories of a chaotic system may coalesce because of finite arithmetic precision. We analyse an example of this phenomenon, showing that it occurs surprisingly frequently. We argue that our model belongs to a universality class of chaotic systems where this numerical coincidence effect can be described by mapping it to a first-passage process. Our results are applicable to aggregation of small particles in random flows, as well as to numerical investigation of chaotic systems.

Keywords: numerical precision, first-passage, chaos

(Some figures may appear in colour only in the online journal)

## 1. Introduction

When we numerically compute two distinct trajectories of a deterministic system, after a certain number of iterations their coordinates may happen to be exactly equal, to machine precision. At this point all subsequent computations of the two trajectories yield exactly the same values. We might say that the trajectories have undergone *numerical coalescence*. This coalescence effect is readily observed in systems with stable dynamics, where nearby trajectories approach each other, typically with an exponentially decreasing separation. It might, however, be expected that it would be unusual to see this numerical coalescence in chaotic systems, where nearby trajectories have an exponentially growing separation (the concept of chaos in the theory of dynamical systems is discussed in [1, 2]).

[3] Author to whom any correspondence should be addressed.

There is a body of literature on the implications of finite numerical precision for investigations of dynamical systems. Most of the works that we have found focus on the statistics of the lengths of periodic orbits of the discrete map which results from using a finite numerical precision. Grebogi, Ott and Yorke [3] characterise the mean length and length distribution of the discretised model, and also the distribution of the number of periodic orbits obtained for a given number of initial conditions. Their work built upon earlier contributions containing partial results [4, 5], and was later developed by numerous other authors ([6–8] are among the most noteworthy contributions). There are a smaller number of works which have addressed the question which we consider, namely, when will two trajectories coalesce due to finite numerical precision. Maritan and Banavar [9] discuss the effects of adding noise to a chaotic dynamical system, showing that there is a 'synchronisation' of different trajectories if the numerical precision is finite. Later, Longa, Curado and Oliveira ([10], see also [11, 12]) explicitly discuss the roundoff-induced coalescence of chaotic trajectories for some specific examples.

Our own work will consider whether and how a universal description of numerical coalescence can be developed. As a first step, we analyse this phenomenon in a simple dynamical system which shows a transition to chaos, exploring its dependence upon the numerical precision of the calculation, which is denoted by $\delta$. In our numerical work we used variable precision arithmetic implemented in the *mpmath* package [13] for the Python programming language, and comparable results were obtained using the Maple mathematical software system [14]. These packages allow the number of decimal digits, $M$, to be set to an arbitrary integer value. If the typical magnitude of the numbers representing the trajectory is $\bar{x}$, we may write

$$\delta \sim \bar{x}\, 10^{-M}. \tag{1}$$

Numerical experiments on a model system, introduced in section 2 below showed that coalescence is surprisingly frequent. In section 3 we explain and demonstrate a simple theory which gives a surprisingly accurate quantitative description of this observation, showing that our numerical results are in agreement with a calculation which maps the numerical coalescence to a first-passage problem [15] for a simple stochastic process. In section 4 we argue that our results are representative of a physically significant universality class of chaotic systems, which combine chaotic dynamics with the influence of external noise. Our theory introduces a universal scaling function which can be used to collapse data on the variation of the mean number of iterations to coalescence as a function of the numerical precision and two parameters describing the instability of the attractor.

As well as being relevant to the numerical exploration of complex dynamical systems, the effect can also serve as a model for aggregation of small particles in complex flows (which seems to have been first considered by Deutsch [16], this problem is reviewed in [17–19]). If the particles aggregate when their separation falls below a threshold, $\delta$, this is analogous to computing trajectories with a finite numerical precision.

Our explanation of the numerical coalescence phenomenon is related to earlier studies [20, 21], where it was shown that trajectories of a chaotic system can display a clustering effect, which is characterised by a power-law distribution of their separations. We review the relationship between the results in this paper and those earlier works in our conclusions, section 5.
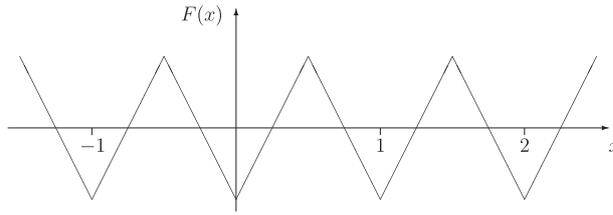
**Figure 1.** Sawtooth function used in equation (2).

## 2. An example

We start with a simple example illustrating the effect that we wish to explain and analyse. Consider trajectories of a one-dimensional map

$$x_{n+1} = x_n + F(x_n - \phi_n) \tag{2}$$

in the case where $F$ is a function which is continuous and differentiable almost everywhere, and which has unit period, $F(x + 1) = F(x)$. The $\phi_n$ are random numbers, chosen independently at each time step, with a distribution which is uniform on $[0, 1]$. These random variables could represent the effects of external noise, or of coupling to other degrees of freedom. We also found it convenient to require that the mean value of $F(x)$ is equal to zero. Note that, while a single trajectory of (2) executes a random walk, this equation describes a differentiable dynamical system, so that it is possible to calculate the Lyapunov exponent [1]. A system with similar properties to (2) is discussed in some detail in [22].

In our study the function $F(x)$ was piecewise linear, having a sawtooth form illustrated by figure 1, with gradients $\pm g$ on intervals of length $1/2$,

$$F(x) = \begin{cases} gx - \dfrac{g}{4} & 0 \leqslant x \leqslant \dfrac{1}{2} \\ g(1 - x) - \dfrac{g}{4} & \dfrac{1}{2} \leqslant x \leqslant 1 \end{cases}. \tag{3}$$

With this choice of $F(x)$, an individual trajectory $x_n$ executes a random walk for which the variance of the step sizes is $g^2/48$, implying that

$$\langle x_n \rangle = 0, \quad \langle x_n^2 \rangle = 2\mathcal{D}n, \quad \mathcal{D} = \frac{g^2}{96}, \tag{4}$$

where $\langle \cdot \rangle$ denotes expectation value.

Because the map is periodic, with period unity, if two trajectories $x_n$ and $x_n'$ differ by an integer, then $x_n - x_n'$ remains equal to the same integer for all subsequent iterations. Note that the map has multiple pre-images when $g > 1$. We shall assume that $g > 1$ throughout our discussion of the map defined by (2) and (3).

In section 3 we demonstrate that the map is chaotic (because the Lyapunov exponent, $\lambda$, is greater than zero [1]) for $g > \sqrt{2}$. When $\lambda > 0$, nearby trajectories should separate exponentially [1]: if $\Delta x_n$ is the separation of two trajectories after $n$ iterations, then

$$\lambda_n = \frac{1}{n} \, \ln \left( \frac{\Delta x_n}{\Delta x_0} \right) \tag{5}$$

**Table 1.** Two trajectories of a realisation of (2) after $n = 2.5 \times 10^5$ iterations, computed with $M = 10$ digit arithmetic. One of the initial conditions was random in [0, 1], and the initial separation was $\Delta x_0 = 0.25$ in all cases.

| $g$ | $x_n$ | $x_n'$ | $\Delta x_n$ |
|------|--------------|--------------|----------------|
| 1.3 | −94.673 871 72 | −93.673 871 72 | −1.0 |
| 1.35 | 41.579 903 09 | 44.579 903 09 | −3.0 |
| 1.4 | 41.417 227 53 | 41.417 227 53 | 0.0 |
| 1.45 | 84.316 049 15 | 84.316 049 15 | 0.0 |
| 1.5 | 46.595 226 84 | 46.595 226 84 | 0.0 |
| 1.55 | 68.706 610 11 | 172.695 6409 | −103.989 0308 |
| 1.6 | −60.552 167 35 | −147.545 1987 | 86.993 0313 |
| 1.65 | −48.663 642 09 | 155.337 1666 | −204.000 8087 |
| 1.7 | −154.982 8462 | −122.617 0971 | −32.365 749 12 |

approaches the Lyapunov exponent $\lambda$ as $n \to \infty$, provided $\Delta x_0$ is sufficiently small that $|\Delta x_n| \ll 1$. When $\lambda < 0$, trajectories converge to the same point (if their initial separation is small) or else to integer separations due to the periodic nature of the one-dimensional map. When $\lambda > 0$, it might be expected that a very small initial separation of trajectories eventually grows to be of order unity, and the similarity of (2) to the equation of a random walk leads one to expect that the subsequent growth of separation is diffusive, $\Delta x \sim \sqrt{n}$.

However, numerical investigations of (2) show a different behaviour. Table 1 lists the separations for pairs of trajectories with $x_0$ random and an initial separation of $\Delta x_0 = 0.25$ after $n = 2.5 \times 10^5$ iterations of the map, for a range of values of $g$. Here we used an arithmetic precision which was defined by specifying $M = 10$ decimal places. The numerically computed separations of the two trajectories, $x_n$ and $x_n'$, are either exactly zero or exactly integers, for two values of $g$ which are in excess of the threshold for chaos, which is at $g = \sqrt{2} = 1.414\,21\ldots$.

It is easy to understand why this numerical coalescence effect is possible for values of $g$ beyond the threshold for chaos. When $\lambda > 0$, it is still possible for trajectories to coalesce if two trajectories happen to reach *exactly* the same point (this is possible because the calculation uses finite precision arithmetic, and because points may have multiple pre-images). However, we might expect that this occurrence is rare. Above the threshold for chaos, nearby points are separating exponentially. If these separations were to fill the unit interval with constant density, there would be a probability $P \sim \delta$ to coalesce at each iteration of the map. If the probability to coalesce were $\delta$ upon each iteration, then after $n$ iterations the probability $P_c$ for the paths to have undergone coalescence would be

$$P_c \sim n\bar{x}\,10^{-M}. \qquad (6)$$

In our numerical investigation illustrated by table 1, $n = 2.5 \times 10^5$, implying (from equation (4), using $g = \sqrt{2}$ as a representative value) that $\bar{x} = \sqrt{2\mathcal{D}n} \approx 100$. This would give an estimate for the probability for coalescence of $P_c \sim 2.5 \times 10^5 \times 100 \times 10^{-10} = 2.5 \times 10^{-3}$. According to this estimate, the results displayed in table 1 appear to be highly unlikely. The remainder of this paper will explain and quantify the effect illustrated in table 1, (section 3), and discuss the extent to which it is a manifestation of a universal phenomenon (section 4).

**Table 2.** Tabulation of the mean number of iterations before coalescence, $\langle N \rangle$, determined numerically for different values of the coefficient $g$ and of the number of digits, $M$. The Lyapunov exponent $\lambda$, given by the first line of equations (9), is positive when $g > \sqrt{2} = 1.41 \dots$.

| | $\langle N \rangle$ | | | | | | |
|---|---|---|---|---|---|---|---|
| $g$ | $M = 7$ | $M = 10$ | $M = 15$ | $M = 20$ | $M = 30$ | $M = 40$ | $M = 50$ |
| 1.25 | 58.0 | 81.8 | 120 | 159 | 237 | 318 | 396 |
| 1.3 | 83.0 | 120 | 177 | 243 | 363 | 481 | 612 |
| 1.32 | 101 | 141 | 217 | 295 | 444 | 599 | 761 |
| 1.34 | 119 | 180 | 273 | 371 | 566 | 773 | 957 |
| 1.36 | 151 | 230 | 371 | 502 | 785 | $1.08 \times 10^3$ | $1.33 \times 10^3$ |
| 1.38 | 193 | 323 | 523 | 739 | $1.17 \times 10^3$ | $1.66 \times 10^3$ | $2.11 \times 10^3$ |
| 1.39 | 227 | 392 | 668 | 957 | $1.61 \times 10^3$ | $2.24 \times 10^3$ | $2.92 \times 10^3$ |
| 1.4 | 272 | 467 | 883 | $1.42 \times 10^3$ | $2.48 \times 10^3$ | $3.54 \times 10^3$ | $4.54 \times 10^3$ |
| 1.41 | 327 | 611 | $1.29 \times 10^3$ | $2.10 \times 10^3$ | $4.41 \times 10^3$ | $6.96 \times 10^3$ | $9.75 \times 10^3$ |
| 1.42 | 413 | 828 | $1.91 \times 10^3$ | $3.73 \times 10^3$ | $1.04 \times 10^4$ | $2.00 \times 10^3$ | $3.02 \times 10^4$ |
| 1.43 | 476 | $1.07 \times 10^3$ | $3.25 \times 10^3$ | $8.34 \times 10^3$ | $2.82 \times 10^4$ | | |
| 1.44 | 604 | $1.68 \times 10^3$ | $5.88 \times 10^3$ | $1.97 \times 10^4$ | | | |
| 1.45 | 815 | $2.42 \times 10^3$ | $1.19 \times 10^4$ | $3.09 \times 10^4$ | | | |
| 1.46 | $1.07 \times 10^3$ | $3.93 \times 10^3$ | $2.41 \times 10^4$ | | | | |
| 1.47 | $1.50 \times 10^3$ | $6.25 \times 10^3$ | $5.75 \times 10^4$ | | | | |
| 1.48 | $1.89 \times 10^3$ | $1.08 \times 10^4$ | $7.57 \times 10^4$ | | | | |
| 1.49 | $2.76 \times 10^3$ | $1.85 \times 10^4$ | $5.73 \times 10^4$ | | | | |

## 3. Coalescence in finite precision arithmetic

### 3.1. Numerical investigation

When two trajectories, started from randomly chosen initial conditions, reach exactly the same coordinate (or else two coordinates with an exactly integer separation), their values remain locked together for all subsequent iterations. If the arithmetic of a numerical iteration of the map has a finite precision, say $M$ decimal places, then this phenomenon of *numerical coalescence* provides an explanation for the effect illustrated in table 1. The principal difficulty is to explain why the effect happens so much more frequently than the simple estimate, equation (6).

We can take two trajectories and determine the 'time' $N$ (that is, number of iterations) for them to coalesce. This will be different for different initial conditions. We should therefore look at the probability $P(N)$, or else at statistics such as the moments $\langle N^j \rangle$. The simplest statistic is just the mean time for coalescence, $\langle N \rangle$, and the remainder of this section is concerned with estimating this quantity.

We investigated the mean number of iterations for coalescence of trajectories $\langle N \rangle$ as a function of $g$ and of the number of decimal digits, $M$. The results are presented in table 2. The initial separation was $\Delta x_0 = 0.1$ in all cases, and for all of the data points we averaged over 1000 realisations, with initial conditions distributed randomly with uniform density on $[0, 1]$.

Note that most of these values of $\langle N \rangle$ are sufficiently small that $\bar{x} \sim \sqrt{2\mathcal{D}\langle N \rangle}$ is not a very large number: for example at $g = 1.4$ and $M = 20$, we found $\langle N \rangle \approx 2500$, implying that $\bar{x} \approx 10$, which indicates that only one of the $M = 20$ digits is required to store the integer part

of $x_n$ leaving 19 digits after the decimal point. For this reason our analysis of these data will make the simplifying assumption that the precision of the calculation, $\delta$, is given by $\delta = 10^{-M}$, where $M$ is the number of digits.

### 3.2. Theory: relation to mean first-passage time

Next we consider how to analyse the results in table 2. Because the map (2) has unit period, two trajectories which have an exactly integer separation maintain the same separation for all subsequent iterations. In this sense, integer separations of trajectories are equivalent to a zero separation, and accordingly we define $\Delta x_n$ as the magnitude of the separation of two trajectories modulo unity. In order to facilitate the calculation of $\langle N \rangle$, the separation of two trajectories, $\Delta x$, is transformed into a logarithmic variable,

$$Z \equiv -\ln |\Delta x|. \tag{7}$$

If trajectories were computed with arbitrary precision, the variable $Z$ would occupy the interval $Z \in [0, \infty)$. When $Z$ is large, the separation of two trajectories is very small, and (at points where the derivative of the map exists) the iteration of $Z$ is described by linearisation of the map, so that

$$Z_{n+1} = Z_n - \ln \left| \frac{\partial x_{n+1}}{\partial x_n} \right|. \tag{8}$$

For the map (2), the dynamics of (8) is Markovian, with displacements $\Delta Z_\pm = -\ln(1 \pm g)$ occurring with random choices of the sign, having probabilities $P_\pm = 1/2$. Because (8) is the equation of a random walk, over many iterations the motion of $Z$ can be modelled by an advection–diffusion equation, with a drift velocity $v$ and a diffusion coefficient $D$ (see [23] for a discussion of the relationships between random walks or Langevin processes and diffusion or Fokker–Planck equations). Note that, from the definition of the Lyapunov exponent $\lambda$ [1], we have $\lambda = -v$. The values of $v$ and $D$ are determined from the statistics of $\Delta Z$: if time is measured by the number of iterations, the drift velocity $v$ and diffusion coefficient $D$ are obtained from

$$v = -\lambda = \langle \Delta Z \rangle = -\frac{1}{2} \left[ \ln(g+1) + \ln(g-1) \right],$$

$$\langle \Delta Z^2 \rangle = \frac{1}{2} [\ln(g+1)]^2 + \frac{1}{2} [\ln(g-1)]^2, \tag{9}$$

$$D = \frac{1}{2} \left[ \langle \Delta Z^2 \rangle - \langle \Delta Z \rangle^2 \right].$$

The first of these relations shows that $\lambda = \ln \sqrt{g^2 - 1}$, which is positive when $g > \sqrt{2}$.

When $\Delta x$ is small, implying that $Z$ is large, the behaviour of $Z$ is determined by the linearised equation of motion, leading to (8). In the vicinity of $Z = 0$, however, $Z$ has complex dynamics which could, in principle, be determined from the equation of motion of $x$, [that is, from equation (2)]. However we can observe that the representative point $Z$ does not pass $Z = 0$, and eventually will leave the region close to $Z = 0$. This implies that the diffusion process can be modelled as having a reflecting barrier at $Z = 0$. If we take account of the coalescence of trajectories due to finite-precision representation of arithmetic, this implies that the separation of trajectories becomes zero when $\Delta x = \delta = 10^{-M}$ where $\delta$ is the floating point precision. At this point, the diffusive model

ceases to be appropriate. We can represent this by introducing an absorbing barrier at a position

$$Z_0 = -\ln\delta = M\ln 10. \tag{10}$$

The mean number of iterations before coalescence, $\langle N \rangle$, is the same as the mean time for first contact with the absorbing barrier in the diffusion process. This quantity is known as the *mean first-passage time*.

### 3.3. Calculation of mean time to coalescence

When considering dispersion over distances which are large compared to the displacement at an individual step of a random walk, the motion can be modelled by a diffusive process. In the limit where the number of decimal places $M$ (and therefore the coordinate $Z_0$ of the absorbing barrier) becomes large compared to the steps described by equation (8), we can therefore use a Langevin equation model, of the form

$$\dot{Z} = -\frac{\mathrm{d}V}{\mathrm{d}Z} + \sqrt{2D}\eta(t) \tag{11}$$

where $V(Z)$ is a potential and $\eta(t)$ is white noise.

There is an extensive literature on the mean first-passage time for diffusive processes [15]. We shall use a standard formula for the mean first-passage time for the Langevin equation. We assume that there is a reflecting barrier at $Z_1$, absorbing barrier at $Z_0$, and particles initially released from $Z_i$. The mean first-passage time is (see [24, 25])

$$\langle T \rangle = \frac{1}{D}\int_{Z_i}^{Z_0}\mathrm{d}x\quad \exp[V(x)/D]\int_{Z_1}^{x}\mathrm{d}y\ \exp[-V(y)/D]. \tag{12}$$

As $Z$ approaches $\infty$, the mean velocity $v$ becomes independent of $Z$, and is equal to $-\lambda$, where $\lambda$ is the Lyapunov exponent. The dynamics of $Z$ is also subject to fluctuations about this mean motion (which are quantified by the diffusion coefficient $D$). If the potential is $V(x) = -vx$, then the drift velocity, $-V'(x)$, is a constant, $v$, as required. The true boundary condition at $Z = 0$ could be modelled more faithfully by introducing a delay time, but we shall assume that using a reflecting boundary at $Z = 0$ is sufficient. We could, in principle, average over the initial conditions by averaging $Z_i$ over the steady-state distribution of $Z$, but again we adopt a simplifying assumption, assuming all of the representative points are injected at $Z_i = 0$ (we expect that this approximation will cause our calculation to overestimate the time taken to reach the absorbing barrier). Defining

$$\alpha = \frac{v}{D} \tag{13}$$

and setting $V(x) = -vx$ in equation (12), we obtain

$$\langle T \rangle = \frac{1}{D}\int_{0}^{Z_0}\mathrm{d}x\ \exp(-\alpha x)\int_{0}^{x}\mathrm{d}y\ \exp(\alpha y). \tag{14}$$

Evaluating the integrals gives

$$\langle T \rangle = \frac{1}{v\alpha}\left[\exp(-\alpha Z_0) - 1\right] + \frac{Z_0}{v}. \tag{15}$$

Noting that the expected number of iterations for path coalescence is $\langle N \rangle = \langle T \rangle$, this can be written in the form

$$\langle N \rangle = \frac{Z_0^2}{D} f(X) \tag{16}$$

where

$$X = \frac{\lambda Z_0}{D} \tag{17}$$

and

$$f(X) = \frac{\exp(X) - 1 - X}{X^2}. \tag{18}$$

Because this approximation assumes $|Z_0| \gg 1$, the predicted values of $\langle N \rangle$ are un-observably large or small unless $g$ is close enough to $g_0 = \sqrt{2}$ that we can make the following two approximations:

$$D \approx D_0 = \frac{[\ln(\sqrt{2} - 1)]^2 + [\ln(\sqrt{2} + 1)]^2}{4} \approx 0.388\,41,$$

$$v \approx \left. \frac{\partial \lambda}{\partial g} \right|_{g=g_0} (g - g_0) = \sqrt{2}(g - g_0), \tag{19}$$

where $g_0 = \sqrt{2}$ is the parameter value for the threshold of chaos, and $D_0$ is the value of the diffusion coefficient at $g_0$. Using these approximations we find

$$\langle N \rangle \sim \frac{(\ln\,10)^2}{D_0} M^2 f(X) \approx 13.65 \times M^2 f(X),$$

$$X = \frac{\sqrt{2}\,\ln\,10}{D_0}(g - \sqrt{2}) \approx 8.384 \times M(g - \sqrt{2}). \tag{20}$$

The function $f(X)$ (defined by (18)) is positive for all real $X$. It implies the following limiting behaviours:

$$\lim_{\lambda \to -\infty} \langle N \rangle \sim \frac{-Z_0}{\lambda},$$

$$\lim_{\lambda \to +\infty} \langle N \rangle \sim \frac{Z_0^2}{D} \frac{\exp(X)}{X^2},$$

$$\lim_{\lambda \to 0} \langle N \rangle \sim \frac{Z_0^2}{2D}. \tag{21}$$

The first of these is what would be expected from the definition of the Lyapunov exponent. The value of $\langle N \rangle$ should not exceed $\delta^{-1} = 10^M$, so that exponential growth in the limit as $\lambda \to \infty$ which is predicted by (21) will only be correct when $g - g_0$ is sufficiently small.

Equation (20) are expected to give an asymptotic approximation to $\langle N \rangle$, which is valid when $M \gg 1$ and $g - \sqrt{2} \ll 1$. We compared this theory against the data tabulated in table 2 by testing whether it would collapse onto a single curve, representing the function $f(X)$. Because of the
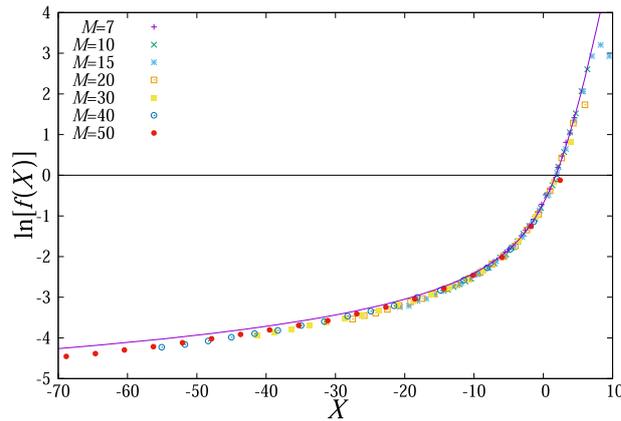
**Figure 2.** Plot $Y$ against $X$ for g from 1.25 to 1.49. Data points for different numbers of digits ($M = 7, 10, 15, 20, 30, 40, 50$), plotted with different symbols according to the legend on the figure, collapse onto the function $\ln\left(\frac{\exp(X)-X-1}{X^2}\right)$ (bold curve).

exponential growth of $f(X)$ for positive $X$, it is more convenient to graph $\ln f(X)$. Accordingly, in order to test the prediction contained in equations (16)–(18), we made a plot of

$$Y = \ln\left(\frac{\langle N \rangle}{13.65 \times M^2}\right) \tag{22}$$

as a function of $X$, as defined by equation (20). In figure 2 we display our plot of $Y$ versus $X$ for the data in table 2. We use different point styles (and colours, online) to distinguish the values of $M$, and included some additional data for more densely sampled values of the coefficient $g$. The points with different colours all collapse onto the same curve, which is well approximated by the function $Y(X) = \ln f(X)$, plotted as a solid curve. This validates the theory described by (16)–(18) as a description of the finite-precision path-coalescence effect for map (2) and (3).

We considered a one-dimensional chaotic system which was designed to enable us to write down an explicit formula for $\langle N \rangle$. We conclude this section by reviewing our calculation, in order to distinguish the important general principles from the specifics of our model system. Our theory, which is contained in equations (16)–(18), uses only the numerical precision $\delta \sim 10^{-M}$ and two additional parameters $\lambda$ and $D$, which characterise the stability of the system. Equations (19) and (20) are descriptions of how these parameters are estimated for our illustrative model system, described by equations (2) and (3). We note that while there were two diffusion coefficients occurring in our calculation, only one of them is directly relevant to the theory. A single trajectory has a diffusive dispersion with diffusion coefficient $\mathcal{D}$, given by equation (4), and the logarithm of the separation of two nearby trajectories is governed by a Markov process, which is approximated by an advection–diffusion equation with diffusion coefficient $D$ and drift velocity $\lambda$ (equation (9)). Not all chaotic systems exhibit diffusive dispersion (see [26]), but this diffusive spatial dispersion of the coordinate $x$ was not a central part of our argument. Our illustrative model was chosen to have diffusive dynamics in order to make the computation of the parameters $\lambda$ and $D$ analytically tractable. The other diffusive process, applying to the logarithmic separation variable $Z$ defined by equation (7), is a generic feature of chaotic dynamical systems. In the next section we discuss the extent to which our approach of modelling numerical coalescence by a first passage process can be generalised.

## 4. Generalisation to other systems

In section 3 we showed that our data on the mean number of iterations before numerical coalescence can be collapsed onto a scaling curve, as illustrated in figure 2. Next we shall argue that the theory for numerical coalescence which was presented in section 3 is applicable to a broad class of dynamical systems, and in this sense it may be said to be 'universal'.

Consider a differentiable map in $d$ dimensions, with a control parameter $g$. We denote phase points on a trajectory by $x_n$, and the small separation of two trajectories at iteration $n$ is denoted by $\delta x_n$. If we define $\delta r_n = |\delta x_n|$ and $Z_n = -\ln \delta r_n$, then when $\delta r_n$ is small, $\Delta Z_n = Z_n - Z_{n-1}$ depends upon the position $x_{n-1}$ and upon the ratios of the components of $\delta x_{n-1}$, but the probability distribution of $\Delta Z_n$ becomes independent of $Z_n$ as $Z_n \to \infty$. Numerical coalescence occurs when $Z_n$ becomes sufficiently large, so that the numerical coalescence process in $d$ dimensions can be formulated as a first-passage problem in one dimension. This one-dimensional problem can be analysed by the approach used in section 3.

We assume that the dynamical system is either autonomous, or else driven by a process which is at least statistically stationary in time. The sequence of values $\Delta Z_n$ has mean and correlation statistics

$$v = \langle \Delta Z_n \rangle,$$
$$C_{nm} = \langle \Delta Z_n \Delta Z_m \rangle - v^2, \tag{23}$$

which are independent of $Z$. If the system has chaotic dynamics, then the $\Delta Z_n$ can be regarded as random variables. Then 'coarse-grained' evolution of $Z$ can be modelled by a Langevin equation, and correspondingly the probability density function $P$ of $\Delta Z$ at iteration $n$ can be modelled by an advection–diffusion equation, where $n$ is identified with the time $t$. The drift velocity is $v$ and the diffusion coefficient $D$ is

$$D = \frac{1}{2} \sum_{m=-\infty}^{\infty} C_{nm}. \tag{24}$$

Note that $-v$ is equal to the leading Lyapunov exponent.

Thus we have argued that the theory presented in section 3 should be quite generally applicable. Its application requires us to identify just two parameters, the Lyapunov exponent $\lambda = -v$ and the diffusion coefficient $D$ from the statistics of the differential of the flow along a trajectory.

Both the Lyapunov exponent and the diffusion coefficient are functions of the control parameter $g$. Our theory is applicable in the vicinity of the transition to chaos, when $g \approx g_0$ defined by $v(g_0) = 0$. We also define

$$v_0' = \frac{\mathrm{d}v}{\mathrm{d}g}\bigg|_{g=g_0}, \quad D_0 = D(g_0). \tag{25}$$

Provided $v_0'$ and $D_0$ are non-zero, we expect that the mean time for coalescence is given by equation (16), where the parameter $X$ is given by

$$X = \frac{g_0' \ln 10}{D_0}(g - g_0)M. \tag{26}$$

We can also relate the scaling parameter $X$ to the correlation dimension $d_2$ of the dynamical system (discussed in [1]). In [20] it is shown that, when $d_2 \ll 1$, $d_2 \sim \lambda/D$, so that

$$X \sim d_2 \ln 10M \sim -d_2 \ln \delta, \tag{27}$$

where $\delta$ is the numerical precision. Hence we find that the relationship between $\langle N \rangle$ and the numerical precision is

$$\langle N \rangle \sim \frac{Z_0^2}{D_0} F(-d_2 \ln \delta)$$

$$= \frac{1}{d_2^2 D_0} \left[ \exp(-d_2 \ln \delta) + d_2 \ln \delta - 1 \right], \tag{28}$$

where $F(\cdot)$ is the function specified by equation (18). In the limit where $X = -d_2 \ln \delta \gg 1$ we therefore have $\langle N \rangle \sim \delta^{-d_2}/D_0$, which is related to an expression for the mean length of a periodic orbit which was proposed in [3].

The theory presented above is expected to be applicable when $D_0$ and $v_0'$ are both non-zero. This is expected to hold when the specification of the dynamical system includes noise, so that the quantities $\Delta Z_n$ are random numbers. The system that we considered in our numerical example, defined by equations (2) and (3), is a concrete example.

In the case of an autonomous dynamical system, however, the assumptions leading to equations (16)–(18) may not hold. In the case where the transition to chaos arises because a stable periodic orbit either disappears, or else undergoes a bifurcation, the $\Delta Z_n$ form a periodic sequence when $g$ is on the stable side of the transition. In this case the diffusion coefficient $D$ is equal to zero in the stable phase, and we must have $D_0 = 0$, so that the theory is not applicable.

## 5. Conclusions

We have exhibited an example of a chaotic system where trajectories coalesce at a surprisingly high rate in the vicinity of the threshold of chaos due to arithmetic truncation errors. The effect was explained by a transformation of the separation of two trajectories to a logarithmic variable, which leads to analogy with a first-passage problem for a diffusive process. This effect is a consequence of transient convergence of chaotic trajectories, which was previously analysed in [20, 21]. Our analysis of the numerical coalescence phenomenon is based upon a principle that was used in those earlier works, namely that the linearised equation of motion is mapped to an advection–diffusion equation if we make a logarithmic transformation, equation (8) in this present work. Here we have shown that the numerical coalescence effect may be understood using a surprisingly simple treatment of the associated first-passage problem.

Our analysis is also relevant to understanding the aggregation of particles in complex flows where the particles aggregate when their separation is equal to $\delta$. In particular, our theory for $\langle N \rangle$ describes the mean time for collision of particles which are advected by a flow which has a Lyapunov exponent which is close to zero.

The theory that we have presented is valid when the stability factors $\Delta Z_n$ have random or pseudo-random fluctuations. This includes almost all real-world applications of chaotic dynamics, where noise will be present. In section 4 we pointed out that the effect may be absent in systems where the transition to chaos arises from perturbation of a periodic orbit.

## Acknowledgments

## ORCID iDs

Bruce N Roth ⬤ https://orcid.org/0000-0003-3414-1541
Michael Wilkinson ⬤ https://orcid.org/0000-0002-5131-9295

## References

[1] Ott E 2002 *Chaos in Dynamical Systems* (Cambridge: Cambridge University Press)
[2] Strogatz S H 2018 *Nonlinear Dynamics and Chaos with Applications to Physics, Biology, Chemistry, and Engineering* 2nd edn (Boca Raton: CRC Press)
[3] Grebogi C, Ott E and Yorke J A 1988 Roundoff-induced periodicity and the correlation dimension of chaotic attractors *Phys. Rev.* A **38** 3688–92
[4] Levy Y E 1982 Some remarks about computer studies of dynamical systems *Phys. Lett.* A **88** 1
[5] Beck C and Roepstorff G 1987 Effects of phase space discretization on the long-time behaviour of dynamic systems *Physica* D **25** 173
[6] Lanford O E III 1998 Informal remarks on the orbit structure of discrete approximations to chaotic maps *Exp. Math.* **7** 317–24
[7] Dellago C and Hoover W G 2000 Finite-precision stationary states at and away from equilibrium *Phys. Rev.* E **62** 6275–81
[8] Wang S, Liu W, Lu H and Kuang J 2004 Periodicity of chaotic trajectories in realizations of finite computer precisions and its implications in chaos communications *Int. J. Mod. Phys.* B **18** 2617–22
[9] Maritan A and Banavar J R 1994 Chaos, noise, and synchronization *Phys. Rev. Lett.* **72** 1451–4
[10] Longa L, Curado E M F and Oliveira F A 1996 Roundoff-induced coalescence of chaotic trajectories *Phys. Rev.* E **54** R2201–4
[11] Longa L, Dias S P and Curado E M F 1997 Lyapunov exponents and coalescence of chaotic trajectories *Phys. Rev.* E **56** 259–63
[12] Dias S P, Longa L and Curado E 2011 Influence of the finite precision on the simulations of discrete dynamical systems *Commun. Nonlinear Sci. Numer. Simulat.* **16** 1574–9
[13] Johansson F 2013 mpmath: a Python library for arbitrary-precision floating-point arithmetic, by Fredrik Johansson and others http://mpmath.org/
[14] Waterloo Maple Inc 2020 Maplesoft https://maplesoft.com
[15] Redner S 2001 *A Guide to First-Passage Processes* (Cambridge: Cambridge University press)
[16] Deutsch J M 1985 Aggregation disorder transition induced by fluctuating random forces *J. Phys. A: Math. Gen.* **18** 1449–56
[17] Falkovich G, Gawedzki K and Vergassola M 2001 Particles and fields in fluid turbulence *Rev. Mod. Phys.* **73** 913–75
[18] Pumir A and Wilkinson M 2016 Collisional aggregation due to turbulence *Annu. Rev. Condens. Matter Phys.* **7** 141–70
[19] Gustavsson K and Mehlig B 2016 Statistical models for spatial patterns of heavy particles in turbulence *Adv. Phys.* **65** 1–57
[20] Wilkinson M, Mehlig B, Gustavsson K and Werner E 2012 Clustering of exponentially separating trajectories *Eur. Phys. J. B.* **85** 18
[21] Pradas M, Pumir A, Huber G and Wilkinson M 2017 Convergent chaos *J. Phys. A: Math. Theor.* **50** 275101
[22] Wilkinson M and Mehlig B 2003 The path-coalescence transition and its applications *Phys. Rev.* E **68** 040101
[23] van Kampen N G 1981 *Stochastic Processes in Physics and Chemistry* 3rd edn (Amsterdam: North Holland)
[24] Lifson S and Jackson J L 1962 On self-diffusion of ions in a polyelectrolyte solution *J. Chem. Phys.* **36** 2410–4
[25] Zwanzig R 1988 Diffusion in a rough potential *Proc. Natl Acad. Sci.* **85** 2029–30
[26] Klages R 2007 *Microscopic Chaos, Fractals and Transport in Non Equilibrium Statistical Mechanics* (Singapore: World Scientific)